Catal Lett (2008) 126:193–199
DOI 10.1007/s10562-008-9606-2

A Mesoporous $Ce_{0.5}Zr_{0.5}O_2$ Solid Solution Catalyst for CO Hydrogenation to iso-C_4 Hydrocarbons

Shaohui Ge · Dehua He · Zhanping Li

Received: 21 April 2008 / Accepted: 29 July 2008 / Published online: 3 September 2008

Abstract Mesoporous $Ce_{0.5}Zr_{0.5}O_2$ solid solution catalyst was synthesized by a sol-gel process using block copolymer Pluronic P123 as the template. The as-prepared catalyst was characterized by X-ray diffraction, H_2-Temperature-programed reduction, BET, and X-ray photoelectron spectra techniques. The catalytic properties of the catalyst were evaluated by the synthesis of iso-C_4 hydrocarbons via CO hydrogenation. The mesoporous catalyst showed much better catalytic selectivity and yield of isobutene and isobutane (i-C_4) from CO hydrogenation at 673–723 K, 5.0 MPa, and 720 h^{-1}, than the solid $Ce_{0.5}Zr_{0.5}O_2$ catalyst prepared by coprecipitation. This was due to the higher BET surface area, pore volume and the reducibility of the mesoporous $Ce_{0.5}Zr_{0.5}O_2$ catalyst.

Keywords $Ce_{0.5}Zr_{0.5}O_2$ · Mesoporous · Isosynthesis · Hydrogenation · Catalyst

1 Introduction

Isosynthesis, referred as the reaction that selectively converts coal or natural gas-derive syn-gas (CO + H_2) to i-C_4 hydrocarbons (isobutene and isobutane), has attracted much attention in recent years because of a world-wide shortage of isobutene and isobutane which are extracted from a limited C_4 stream of a petroleum cracking process at the present time [1]. It has been pointed that zirconia (ZrO_2) was the most selective catalyst for isosynthesis [2, 3]. Another oxide catalyst, ceria (CeO_2), was also selective to isobutene in C_4 hydrocarbons [4]. Then, the ZrO_2 catalyst doped by CeO_2 for promoting i-C_4 selectivity in the isosynthesis via CO hydrogenation was prepared by coprecipitation [5, 6]. It was found that the incorporation of CeO_2 with ZrO_2 (Ce/Zr = 1, molar ratio) changed the redox and acid-base properties of ZrO_2-based catalysts and subsequently affected the catalytic performance [5]. The CeO_2–ZrO_2 sample above was composed of spherical solid nanoparticles. Recently, CeO_2–ZrO_2 oxides in an ordered mesoporous structure are expected to provide enhanced catalytic performance due to their large surface area and a certain degree of size and shape selective. For example, the mesoporous $Ce_{1-x}Zr_xO_2$ ($0 < x < 1$) solid solutions with cubic structure were used to prepare the corresponding $Pd/Ce_{1-x}Zr_xO_2$ ($0 < x < 1$) for CO conversion [7].

For the isosynthesis of i-C_4 hydrocarbons, the $Ce_{0.5}Zr_{0.5}O_2$ showed the highest selectivity and yield among various $Ce_{1-x}Zr_xO_2$ ($0 < x < 1$) solid solutions catalysts prepared by coprecipitation [5, 7–10]. In this paper, a mesoporous $Ce_{0.5}Zr_{0.5}O_2$ was synthesized by a sol-gel process using block copolymer Pluronic P123 as the template according to [11]. For comparison, the solid $Ce_{0.5}Zr_{0.5}O_2$ catalyst prepared by coprecipitation was also prepared. The as-prepared catalysts were evaluated by the synthesis of iso-C_4 hydrocarbons via CO hydrogenation.

2 Experimental

2.1 Catalyst Preparation

The mesorporous $Ce_{0.5}Zr_{0.5}O_2$ solid solution was synthesized by a sol-gel method using block copolymer Pluronic

S. Ge · D. He (✉) · Z. Li
Innovative Catalysis Program, Key Lab of Organic Optoelectronics & Molecular Engineering of Ministry of Education, Department of Chemistry, Tsinghua University, Beijing 100084, China
e-mail: hedeh@mail.tsinghua.edu.cn

P123 as the template and ceric nitrate and zirconium oxide chloride as the precursors [11]. In a typical synthesis, 2.0 g Pluronic P123 was dissolved in 20 mL ethanol, and 2.5 mmol $Ce(NO_3)_3{\cdot}6H_2O$ and 2.5 mmol $ZrOCl_2$. The resulting solution was stirred for 4 h and then transferred to an oven at 313 K. After 48 h aging, the gel product was dried at 363 K for 24 h. Calcination was carried out by slowly increasing temperature from room temperature to 773 K (1 K/min) and heating at 773 K for 6 h. The as-prepared sample was signed as fresh $Ce_{0.5}Zr_{0.5}O_2$ (M). ZrO_2 or CeO_2 solid solution was synthesized by the above sol-gel method by using 5.0 mmol $Ce(NO_3)_3{\cdot}6H_2O$ or 5.0 mmol $ZrOCl_2$ only.

The solid $Ce_{0.5}Zr_{0.5}O_2$ solid solution was synthesized by adding dropwise a solution of $ZrOCl_2$ (0.075 M) and $Ce(NO_3)_3{\cdot}6H_2O$ (0.075 M) into a well-stirred ammonium solution (2.5%) at room temperature. The pH value during precipitation was carefully controlled at 10. The gel was dried at 378 K for 24 h and then calcined at 823 K for 5 h in air. The as-prepared sample was signed as fresh $Ce_{0.5}Zr_{0.5}O_2$ (S).

2.2 Catalyst Characterization

The morphology, physical properties, and phase structure of the prepared catalysts were characterized by several analytical methods. The XRD patterns were recorded on a D/max/RB X-ray diffractometer (Cu Kα, $\lambda = 1.54178$Å). The surface area was measured using the BET method by N_2 physisorption at 373 K on the automatic surface area and pore size analyzer (Autosorb-1-MP 1530 VP).

Temperature-programed reduction (TPR)studies were carried out in a conventional system(flow-type) equipped with a thermal conductivity detector (TCD). The amount of catalyst used was 100 mg in all cases. The catalyst samples were treated in a highly pure Ar at 873 K for 0.5 h before TPR was performed. TPR was carried out in a flow of 5% H_2/Ar (20 mL/min) at a heating rate of 10 K/min. A cold trap (203 K) was placed before the TCD to remove water produced during the reduction. The hydrogen consumption was calibrated using TPR of copper oxide (CuO) under the same conditions. To study the redox properties $Ce_{0.5}Zr_{0.5}O_2$ samples, $Ce_{0.5}Zr_{0.5}O_2$ (M) and $Ce_{0.5}Zr_{0.5}O_2$ (S) samples reoxidized by oxygen after hydrogen reduction were prepared. The $Ce_{0.5}Zr_{0.5}O_2$ was calcined at 823 K in air for 5 h (denoted as "calcined $Ce_{0.5}Zr_{0.5}O_2$"). The calcined $Ce_{0.5}Zr_{0.5}O_2$ was heated in a flow of H_2 (1%) in Ar (25 mL/min) at 1,273 K for 5 h, and the obtained powder was reoxidized in an oxygen flow (25 mL/min) at 873 K for 5 h. This sample was denoted "reduced/reoxidized $Ce_{0.5}Zr_{0.5}O_2$". The TPR experiments on the fresh $Ce_{0.5}Zr_{0.5}O_2$ (M) and $Ce_{0.5}Zr_{0.5}O_2$ (M) samples without Ar treatment at 873 K were also carried".

The acid-base properties of the catalysts were measured by temperature-programed desorption of ammonia(NH_3-TPD) and carbon dioxide(CO_2-TPD), respectively. TPD experiments were carried out in a flow-type apparatus at atmospheric pressure. Typically, a 100-mg sample was treated at its calcined temperature (823 K) in a highly pure helium flow for 0.5 h and then saturated with a 1.0% NH_3/He mixture or highly pure CO_2 flow after cooling to 373 K. After being flushed with He at 373 K for 1 h to remove physisorbed NH_3 or CO_2, the sample was heated to 823 K at a rate of 20 K/min in a helium flow (60 mL/min). The desorbed NH_3 or CO_2 was measured by a Chem3000.

The characterization by means of transmission electron microscope (TEM) was carried out with a JEM-2010 microscope. The accelerating voltage was 120 kV. X-ray photoelectron spectra were analyzed on a PHI-6100 spectrometer (USA) using Mg Ka radiation for exciting photoelectrons. X-ray source was operated at an accelerating voltage of 15 kV and 250 W. The pressure in the ion-pumped analysis chamber was maintained at 1.1×10^{-7} Pa during data acquisition. All binding energies (BE) were referenced to the adventitious C 1 s line at 284.6 eV.

2.3 Isosynthesis Reactions

The hydrogenation of CO was carried out in one specially designed high-pressure flow fixed-bed reactor at 5.0 MPa, 673–723 K, and 720 h^{-1}. The palletized catalyst (1 g) was crushed and sieved to particles (20–40 mesh) and then packed in the reactor. Before the reaction was conducted, the catalyst was pretreated in a stream of N_2 at 673–723 K. Then syn-gas ($CO/H_2 = 1$) was introduced into the reactor. Synthesis gas ($CO/H_2 = 1$) was purified by removing metal carbonyls and water with an activated charcoal trap and a molecular sieve trap, respectively. The reactor effluent was reduced to atmospheric pressure and then injected into two on-line gas chromatographs. One equipped with TCD was used to separate CO, CH_4, CO_2, H_2O, CH_3OH, and CH_3OCH_3 through a GDX-101 column, and another equipped with FID and a 30 m × 0.53 mm Al_2O_3 capillary column was applied to separate hydrocarbons. The calculations of CO_2 selectivity and yield were based on the net formation amount of CO_2 in the reaction, which was obtained by subtracting the CO_2 quantity in the reactant stream from that in the products. In all experiments the mass balances in carbon and oxygen were within ± 2%.

3 Results and Discussion

Figure 1 shows the wide-angle X-ray diffraction (PXRD) pattern of mesoporous solid solution sample $Ce_{0.5}Zr_{0.5}O_2$(M). It suggests the nanocrystalline nature of the

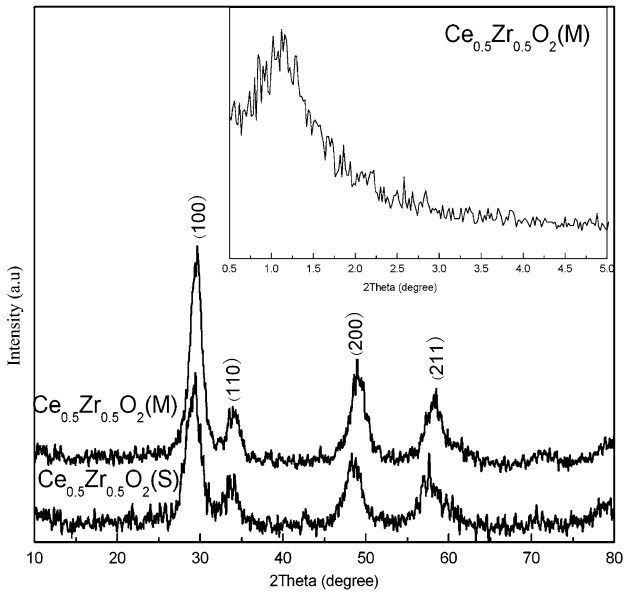

Fig. 1 Wide-angle PXRD pattern of $Ce_{0.5}Zr_{0.5}O_2$. Insert: small-angle PXRD pattern

as-prepared sample is the same as the $Ce_{0.5}Zr_{0.5}O_2$(S). The insert in Fig. 1 presents the small-angle PXRD pattern of the sample. A sharp diffraction peak appears around 1.1° due to (100) plane [8]. The result showed that the as-prepared $Ce_{0.5}Zr_{0.5}O_2$(M) sample was a solid solution and had mesoporous structure. Figure 2 shows the XRD patterns of $Ce_xZr_{1-x}O_2$ ($x = 0$, 0.33, 0.5, 0.67 and 1) samples synthesized form the sol-gel method. A monoclinic phase with the peaks at $2\theta \sim 28.4°$ and 31.5° is the dominating crystal phase in pure ZrO_2. When 33% Zr^{4+} was replaced by Ce^{4+}, the crystal phase of ZrO_2 changed greatly. The diffraction peaks at $2\theta \sim 28.4^o$ and 31.5^o disappeared while the peak at $2\theta \sim 29.6^o$ appeared. It should be assigned to a tetragonal or/and cubic ZrO_2 phase [5, 6]. For a tetragonal ZrO_2 phase, the peaks at $2\theta \sim 30.2$, 34.8, and 35.2° are the characteristic peaks, but for cubic ZrO2, its characteristic peaks also appear at $2\theta \sim 30.2$ and 34.8° [5]. Figure 2 shows only four weak and board diffraction peaks for the $Ce_xZr_{1-x}O_2$ ($x = 0.33$, 0.5 and 0.67) samples, and it is difficult to discern a tetragonal phase from a cubic phase. However, from our previous work [5, 6], the $Ce_xZr_{1-x}O_2$ was assigned to a pseudo-cubic tetragonal phase by Raman spectra. With increasing the content of Ce, the 2θ (values) of the four peaks observed decreased slightly, but they were still higher than those of pure CeO_2 samples. It is evident that the CeO_2 and ZrO_2 formed a solid solution because a free CeO_2 and ZrO_2 phase are not observed [5].

Figure 3 shows the BET nitrogen adsorption–desorption isotherm of the samples after clacination. The isotherm can be ascribed to type IV with H1-shaped hysteretic loops, implying the presence of cylindrical pores [11, 12]. The BET surface area of the crystalline mesoporous solid solution $Ce_{0.5}Z_{r0.5}O_2$ (M) gave a value of 255 m^2/g, much higher than that of solid sample $Ce_{0.5}Z_{r0.5}O_2$ (S) obtained by coprecipitation, as shown in Table 1. The crystal size of $Ce_{0.5}Z_{r0.5}O_2$ (M) was 7.8 nm, larger than that of $Ce_{0.5}Z_{r0.5}O_2$ (S) as shown in Table 1. The particle size of samples from TEM characterization obtained was similar. The result indicates that the $Ce_{0.5}Z_{r0.5}O_2$ (S) has a smaller crystallize size, but low surface area. This was probably

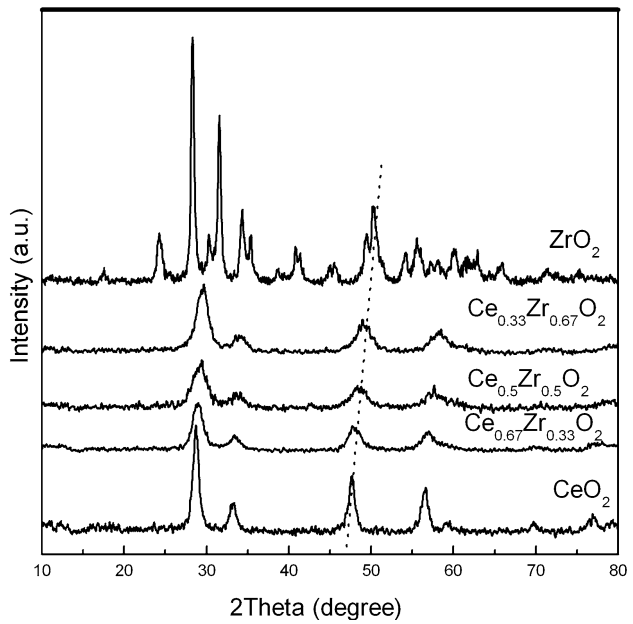

Fig. 2 XRD patterns of $Ce_xZr_{1-x}O_2$ solid solutions

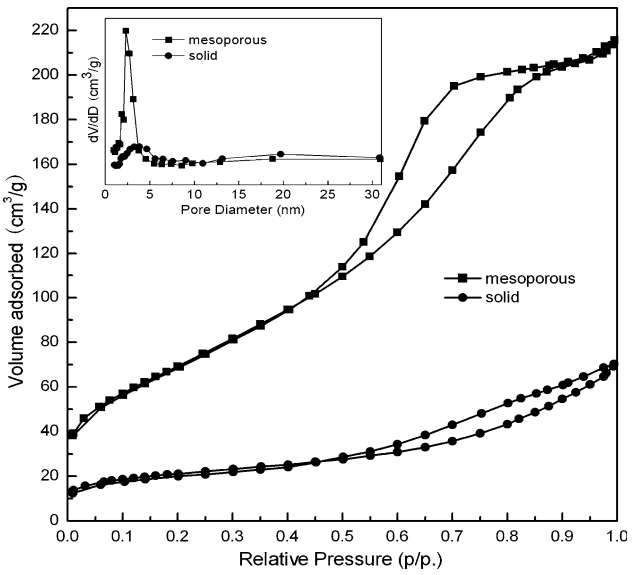

Fig. 3 Nitrogen adsorption–desorption isotherms of mesostructured $Ce_{0.5}Zr_{0.5}O_2$. Inset: corresponding pore size distribution curves deduced form the desorption branches

Table 1 Properties of $Ce_{0.5}Zr_{0.5}O_2$ solid solutions

Samples	S_{BET} (m^2/g)	Cummulative pore volume (cm^3/g)[a]	Average pore diameter[b] (nm)	Base site/acid site ratio	Particle size (nm)[c]	
					A	B
Mesoporous	255	0.349	2.3	1.9	7.8	8.2
Solid	73	0.101	3.8	1.6	6.6	8

[a] BJH desorption cumulative pore volume of pores in the range 1.7–300 nm

[b] BJH desorption average pore diameter

[c] The particle size was obtained by XRD (A) and TEM (B)

due to significantly less cumulative pore volume compared with $Ce_{0.5}Zr_{0.5}O_2$ (M) [6]. The pore volume of mesoporous $Ce_{0.5}Zr_{0.5}O_2$ (M) sample was two times more than solid $Ce_{0.5}Zr_{0.5}O_2$ (S) sample, and the mesoporous $Ce_{0.5}Zr_{0.5}O_2$ (M) sample had a narrow range of pore size. It shows that the increasing of surface area of $Ce_{0.5}Zr_{0.5}O_2$ (M) is ascribed to its mesoporous structure.

An X-ray photoelectron spectrum is a powerful technique for surface compositional analysis of nano-materials. Figure 4 reveals the presence of cerium, zirconium, and oxygen on the surface of $Ce_{0.5}Zr_{0.5}O_2$ catalysts. The Ce 3d XPS BE of the catalysts showed six peaks at about 882.5, 888.9, 898.6, 900.9, 907.6 and 916.8 eV, which was consistent with that of Ce^{4+} species, indicating that the main valence of cerium in $Ce_{0.5}Zr_{0.5}O_2$ was +4. The overlapping peaks at about 181.8 and 184.2 eV corresponded to the spectra of Zr $3d_{5/2}$ and Zr $3d_{3/2}$ were observed. The binding energy of O 1 s was approximately 529.7 eV, which was assigned to the lattice oxygen associated with metal oxides. A broad shoulder at higher BE region might be attributed to the oxygen in hydroxyl groups. The results imply that the surface species of Ce, Zr, and O elements over both

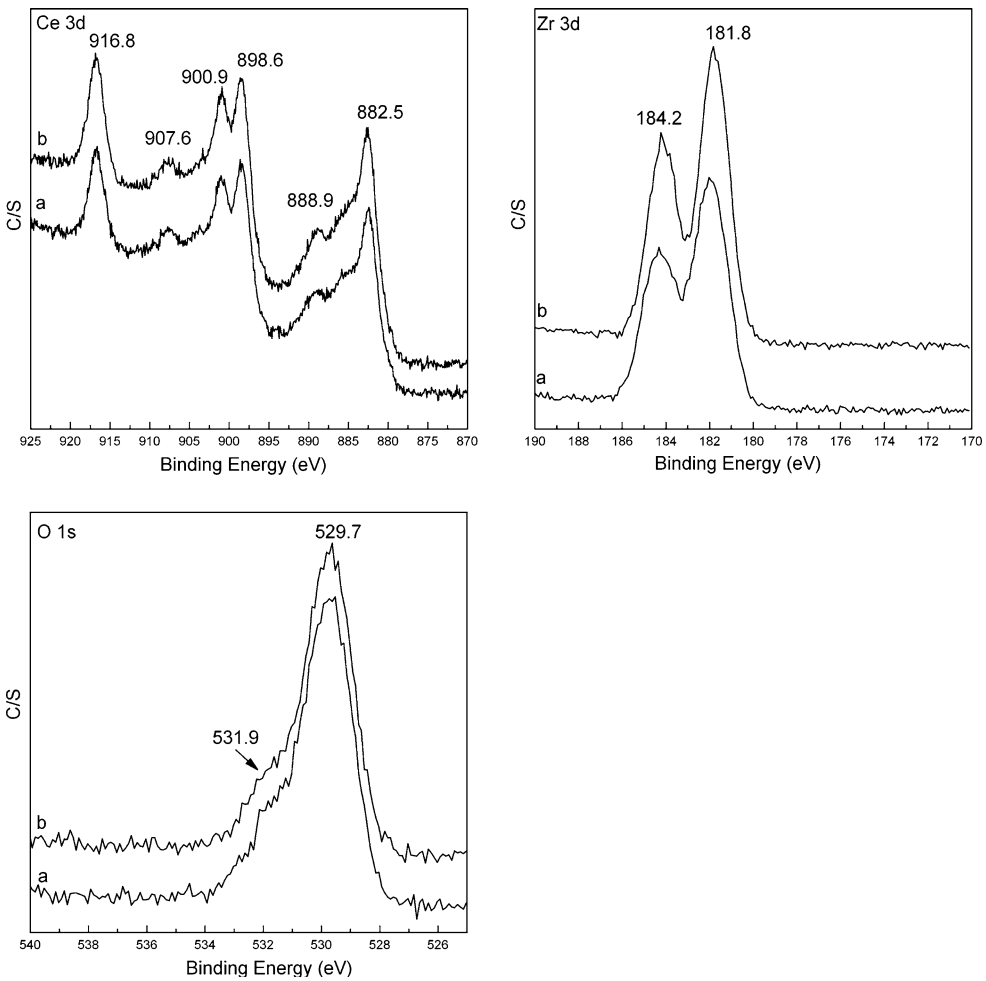

Fig. 4 XPS spectra of samples. (**a**) $Ce_{0.5}Zr_{0.5}O_2$ (M) and (**b**) $Ce_{0.5}Zr_{0.5}O_2$ (S)

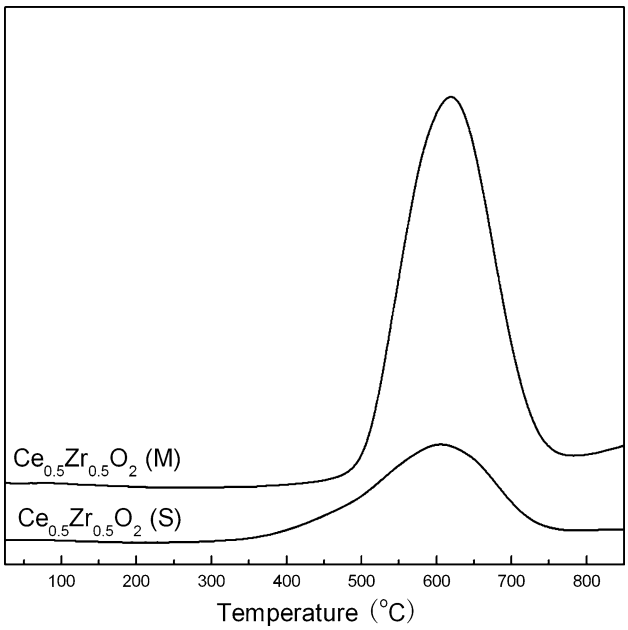

Fig. 5 H_2-TPR profiles of $Ce_{0.5}Zr_{0.5}O_2$ samples

$Ce_{0.5}Zr_{0.5}O_2$ (M) and $Ce_{0.5}Zr_{0.5}O_2$ (S) were the same [13]. Figure 5 shows the TPR results of the $Ce_{0.5}Zr_{0.5}O_2$ samples. It can be seen that both $Ce_{0.5}Zr_{r0.5}O_2$ (M) and $Ce_{0.5}Zr_{r0.5}O_2$ (S) exhibited one peak around 600 °C. This implies that the species and the strength of lattice oxygen were the same for both catalysts [14, 15]. Table 2 shows the H_2 consumption over different $Ce_{0.5}Zr_{r0.5}O_2$ samples. The fresh $Ce_{0.5}Zr_{r0.5}O_2$ (M,S) samples without heating treatment before TPR experiments have much higher amount of H_2 consumption than calcined samples. The "reduced/reoxidated $Ce_{0.5}Zr_{0.5}O_2$" samples possessed more amount of H_2 in TPR consumption than calcined samples. The results showed that the pretreatment of the samples by Ar could delete oxygen from the support. The amount of H_2 consumption in TPR for $Ce_{0.5}Zr_{0.5}O_2$ (M) was much higher than that for $Ce_{0.5}Zr_{0.5}O_2$ (S), and the $Ce_{0.5}Zr_{0.5}O_2$ (M) could be reduced more easily [16, 17]. This enhancement of H_2 consumption might be due to the increase of surface area and pore structure of $Ce_{0.5}Zr_{0.5}O_2$ (M).

Table 2 The surface properties of samples

Samples	Treatment	H_2-consumptions (μmol/g)
Mesoporous	Fresh	1,481
Mesoporous	Calcined	752
Mesoporous	Reduced/reoxidated	1,171
Solid	Fresh	1,284
Solid	Calcined	118
Solid	Reduced/reoxidated	1,018

For the isosynthesis, the activities of ZrO_2 and CeO_2 were depended on the surface area of oxides or/and the acid-base properties [6]. The ZrO_2 has high amount of acid and base sites, and was pointed to be excellent selective catalyst in the isosynthesis [2, 3]. The CeO_2 showed a higher activity than ZrO_2 due to the difference of crystal phase [6]. As shown in Table 3, both ZrO_2 and CeO_2 showed activities in the isosynthesis at 673–723 K and 5 MPa. The CO conversions increased with the increase of reaction temperatures in the range of 673–723 K over both ZrO_2 and CeO_2 catalysts. CeO_2 exhibited high selectivity of hydrocarbons at 673 K, but it decreased with the increase of temperatures from 673 to 723 K. The major role of cerium oxide in the catalysts is to control the oxygen concentration by storage and release under the reaction environment [18]. However, as a support, ceria will result in significant efficiency decrease of the catalysts under thermally harsh environment [13]. Much attention has been focused on Ce-Zr mixed oxide [19–22]. In the mixed oxide $Ce_xZr_{1-X}O_2$, Zr^{4+} ion partially substitutes for Ce^{4+} in the lattice of CeO_2, forming a solid solution. Compared to pure ceria, such solid solution maintains the reversible Ce^{3+}/Ce^{4+} redox property even after exposure to the reduction condition above 1,173 K [13, 20] and show the improved thermal resistance and better catalytic oxidation activity at higher temperature [21, 22]. It has been reported that the incorporation of CeO_2 into ZrO_2 greatly enhanced the reduction behavior and/or the acid-base properties [6]. The changing trends that the ratio of i-C_4/n-C_4 increases with increasing ratio of base/acid sites have been found [5, 8]. Table 1 shows the ratios of base sites/acid sites of both $Ce_{0.5}Zr_{0.5}O_2$ (M) and $Ce_{0.5}Zr_{0.5}O_2$ (S) catalysts. The $Ce_{0.5}Zr_{0.5}O_2$ (M) sample had a higher ratio, and showed a high ratio of i-C_4/CH ratio as shown in Table 3. It was suggested that differences in both acid and base sites can be attributed to the various fractions of crystal phases along with the crystallite sizes of catalyst [6]. The $Ce_{0.5}Zr_{0.5}O_2$ (M) and $Ce_{0.5}Zr_{0.5}O_2$ (S) catalysts have the same crystal phase and similar crystallite sizes, and the different base/acid site should be attributing to difference in BET surface area [6]. On the other hand, i-C_4 selectivity in the isosynthesis was increased with the H_2 consumption of ZrO_2 based catalysts in the TPR characterization. For the isosynthsis, there are two independent paths, CO insertion and condensation reaction, for the chain propagation reactions leading to C_{2+} hydrocarbons over ZrO_2 based catalysts [23, 24]. The CO insertion step comprises the addition of a CO molecule into the Zr–C bond of surface aldehyde intermedia. Hence, the product distribution should be that which could be predicted from a typical S–F-A distribution. The condensation reaction comprises the condensation of a surfacebound enolate with a surface alkoxy contributes to C_4 and C_{4+} products. The

Table 3 Comparable catalytic performances of mesoporous and solid $Ce_{0.5}Zr_{0.5}O_2$ catalysts in the isosynthesis at different temperatures[a]

T (K)	CO conversion (%)	Selectivity (C mol%)		Distribution of hydrocarbons (C mol%)					i-C_4/CH (C mol%)[g]	i-C_4 yield %
		CH[f]	CO_2	C_1	C_2	C_3	C_4	C_{5+}		
673[b]	21.1	48.7	51.3	14.3	7.4	4.9	63.6	9.8	55.4	5.7
673[c]	8.7	51.1	48.9	14.2	6.5	13.3	51.5	14.4	41.6	3.6
673[d]	18.14	80.6	19.4	21.0	13.2	11.0	52.3	2.5	46.78	6.8
673[e]	14.91	58.8	41.2	14.8	6.8	8.5	58.7	11.2	47.06	4.1
698[b]	34.9	63.6	36.4	16.4	6.3	6.5	61.1	9.7	49.2	10.9
698[c]	11.1	54.3	45.7	13.5	6.7	19.6	50.2	10.0	40.5	4.5
698[d]	20.46	72.6	27.4	27.5	7.6	7.9	52.5	4.5	48.25	7.2
698[e]	17.69	60.5	39.5	17.6	19.3	8.2	50.5	4.4	44.15	4.7
723[b]	37.4	88.9	11.1	20.1	7.7	6.7	58.8	6.7	45.0	15.0
723[c]	21.2	58.3	41.7	14.1	8.1	25.3	43.5	9.1	34.2	7.3
723[d]	25.82	68.6	31.4	29.4	8.1	10.7	47.2	4.6	43.92	7.8
723[e]	19.27	70.0	30.0	23.2	15.9	7.8	49.3	3.8	43.01	5.8

[a] Reaction conditions: 5.0 MPa, GHSV = 720 h^{-1}, $CO/H_2 = 1$

[b] Mesorporous $Ce_{0.5}Zr_{0.5}O_2$ solid solution

[c] $Ce_{0.5}Zr_{0.5}O_2$ solid solution prepared by coprecipitation

[d] CeO_2

[e] ZrO_2

[f] Hydrocarbons

[g] i-C_4 selectivity in total hydrocarbons

enhancement of H_2 consumption was ascribed to an increase of the lattice oxygen mobility in the bulk of $Ce_{0.5}Zr_{0.5}O_2$ solid solution because of the distortion of the ZrO_2 structure by the incorporation of CeO_2 and then the lattice oxygen would be more active to react with H_2 [25].

The i-C_4 selectivity could be affected by the redox property of the CeO_2–ZrO_2 catalysts [5]. This suggests that the enhancement of H_2 consumption, the mobility of lattice oxygen, could affect the formation of the intermedia substances for the condensation reaction, η^3—enolate and methoxy species [13] and then promoted the i-C_4 selectivity [5]. Table 3 shows that the quantity of H_2 consumption increased greatly after changing the structure of $Ce_{0.5}Zr_{0.5}O_2$ from solid to mesoporous. This might be due to its high surface area, pore volume, the ratio of base/acid site ratio as shown in Fig. 3 and Table 1. The catalytic performance of the $Ce_{0.5}Zr_{0.5}O_2$ (M) and $Ce_{0.5}Zr_{0.5}O_2$ (S) catalysts in the isosynthesis are shown in Table 3. The predominant reaction products consisted of hydrocarbons and CO_2. Among the four catalysts ($Ce_{0.5}Zr_{0.5}O_2$ (M), $Ce_{0.5}Zr_{0.5}O_2$ (S), CeO_2 and ZrO_2), the catalytic activity and selectivity of C_4 hydrocarbons over mesoporous $Ce_{0.5}Zr_{0.5}O_2$ (M) catalyst was highest under the same reaction conditions. It is obvious that the CO conversion over mesoporous catalyst $Ce_{0.5}Zr_{0.5}O_2$ (M) was 10–24% higher than that of solid catalyst $Ce_{0.5}Zr_{0.5}O_2$ (S). The CO conversion over $Ce_{0.5}Zr_{0.5}O_2$ (M) was also promoted by increasing temperatures. The selectivity of hydrocarbons and the CO_2 selectivity increased with the increase of reaction temperature over $Ce_{0.5}Zr_{0.5}O_2$ (M) catalyst. On the other hand, the selectivity of CO_2 over meosoporous catalyst $Ce_{0.5}Zr_{0.5}O_2$ (M) was much lower than that of solid catalyst $Ce_{0.5}Zr_{0.5}O_2$ (S). The highest selectivity of hydrocarbons and lowest CO_2 selectivity were obtained at 723 K over $Ce_{0.5}Zr_{0.5}O_2$ (M) catalyst. For the meosoporous catalyst $Ce_{0.5}Zr_{0.5}O_2$ (M), more CO and H_2 could be absorbed on the active sites due to its meosoporous pores [26], which would increase the catalytic activity. Then the increase concentration of CO absorbed also promotes the formation of alkene and the growth of C–C chains [26, 27]. Thus, the selectivity of alkane and alkene is promoted by the meosoporous. Moreover, the bulk density of meosoporous catalyst was 1.2 g/mL, much smaller than that of solid catalyst (2.1 g/mL).

4 Conclusion

Mesoporous $Ce_{0.5}Zr_{0.5}O_2$ solid solution catalyst was synthesized by a sol-gel process using block copolymer Pluronic P123 as the template. Its mesoporous structure was confirmed by XRD pattern. The mesoporous $Ce_{0.5}Zr_{0.5}O_2$ (M) exhibits higher BET surface area, pore volume, and the reducibility than the solid $Ce_{0.5}Zr_{0.5}O_2$(S) catalyst prepared by coprecipitation. Thus, it shows better catalytic properties in the isosynthsis of iso-C_4

hydrocarbons. The as-prepared mesoporous $Ce_{0.5}Zr_{0.5}O_2$ (M) catalyst showed 37.4% CO conversion, 88.9% hydrocarbon selectivity and 15% i-C_4 yield.

Acknowledgment This work was supported by National Natural Science Foundation of China (Grant No: 20590362 and 20373031) and Ministry of Science and Technology of China (Grant No: 2007AA05Z332).

References

1. Sofianos A (1992) Catal Today 15:149
2. Pichler H, Ziesecke KH (1949) Brennst Chem 30:13
3. Pichler H, Ziesecke KH, Traeger B (1949) Brennst Chem 30:333
4. Maruya K, Ito K, Kushihashi K, Kishida Y, Domen K, Onishi T (1992) Catal Lett 14:122
5. Li YW, He DH, Zhu QM, Zhang X, Xu BQ (2004) J Catal 221:584
6. Khaodee W, Jongsomjit B, Assabumrungrat S, Praserthdam P, Goto S (2007) Catal Commun 8:548
7. Huo C, Yu JC, Wang X, Lai S, Qiu Y (2005) J Mater Chem 15:2193
8. Li YW, He DH, Cheng ZX, Su CL, Li JR, Zhu QM (2001) J Mol Catal 175(1/2):267
9. Li YW, He DH, Gee SH, Zhang RJ, Zhu QM (2008) Appl Catal B 80:72–80
10. Li YW, He DH, Zhu ZH, Zhu QM, Xu BQ (2007) Appl Catal 319:119–127
11. Yuan Q, Liu Q, Song WG, Feng W, Pu WL, Sun LD, Zhang YW, Yan CH (2007) J Am Chem Soc 129:6698
12. Sing KAW, Everett D, Hual RAW, Pierotti RA, Rouquerol J, Siminiewska T (1985) Pure Appl Chem 57:603
13. Wang SP, Zhang TY, Su Y, Wang SR, Zhang SM, Zhu BL, Wu SH (2007) Catal Lett 121:70
14. Otsuka K, Wang Y, Nakamura M (1999) Appl Catal A Gen 183:317
15. Fornasiero P, Balducci G, Monte R, Kašpar J, Sergo V, Gubitosa G, Ferrero A, Graziani M (1996) J Catal 164:173
16. Masui T, Peng YM, Machida KI, Adachi GY (1998) Chem Mater 10:4005
17. Wang RG, Crozier PA, Sharma R, Adams JB (2008) Nano Lett 8:962
18. Monte RD, Kaspar J (2005) Catal Today 100:27
19. Liu X-Y, Wang S-D, Yuan Z-S, Zhou J, Liu N, Zhang C-X, Fu GZ (2004) Chin J Catal 2:91
20. Kakuta N, Ikawa S, Eguchi T, Murakami K, Ohkita H, Mizushima T (2006) J Alloy Compd 1078:408–412
21. Wang S-P, Zheng X-C, Wang X-Y, Wang S-R, Zhang S-M, Yu L-H, Huang W-P, Wu S-H (2005) Catal Lett 105:163
22. Terribile D, Trovarelli A, Llorca J, Leitenburg CD, Dolcetti G (1998) Catal Today 43:79
23. Jackson NB, Ekerdt JG (1986) J Catal 101:90
24. Tseng SC, Jackson NB, Ekerdt JG (1988) J Catal 109:284
25. Vlaic G, Fornasiero P, Geremia S, Kaspar J, Graziani M (1997) J Catal 168:386
26. Subramaniam B (2001) Appl Catal A Gen 212:199–213
27. Lang X, Akgerman A, Bukur D (1995) Ind Eng Chem Res 34:72–77